Analytical Results on a Chaotic Piecewise-Linear O.D.E.

B. Uehleke and O. E. Rössler
Institute for Physical and Theoretical Chemistry, University of Tübingen

Z. Naturforsch. **39 a**, 342–348 (1984); received December 21, 1983

A variant to the well known Danziger-Elmergreen equation of hormonal regulation is analyzed geometrically by analytical methods. The new method of Poincaré half maps is employed. Several chaotic regimes are found.

1. Introduction

Recently, a piecewise-linear 3-dimensional system with smooth (C^1) trajectories was proposed as a prototypic system for the analytic study of chaotic behavior in three dimensions [1]. Piecewise linear systems form an especially simple class of nonlinear systems. In contrast to other nonlinear systems, the flows can be obtained by analytical methods in these systems.

The method of Poincaré "half maps" is appropriate and was recently applied to the study of a completely linear system [2]. Half maps are defined by a first intersection of a trajectory with an arbitrarily chosen Poincaré surface and the same trajectory's very next passage (in the opposite direction) through the same surface. In the case of a piecewise-linear system, the Poincaré surface will be so chosen as to be identical with the (usually planar) set that separates the two linear half systems.

In the following we present analytical results on a variant of the well-known Danziger-Elmergreen system of hormonal regulation [3], thereby extending earlier results of Cronin [4].

2. The System

We consider the following single-loop feedback system [1]

$$\begin{aligned} \dot{x} &= -x + f(z)\,, \\ \dot{y} &= x - y\,, \\ \dot{z} &= y - z \end{aligned} \tag{1}$$

Reprint requests to Dr. Dr. B. Uehleke, c/o Winthrop GmbH, Am Forsthaus Gravenbruch, 6078 Neu-Isenburg, West Germany.

with the continuous piecewise-linear feedback function

$$f(z) = \begin{cases} Gz - G\,, & \text{for} \quad z \leqq 1\,, \\ Fz - F\,, & \text{for} \quad z > 1\,, \end{cases} \tag{2}$$

and the parameters $G < 0$ and $F > 1$. Danziger and Elmergreen [3] also used (1), but with more parameters allowed in (1), and – on the other hand – with a simpler feedback function ($F = 0$). The constants which were set equal to unity in (1) can be given arbitrary values in general.

Any feedback function $f(z)$ that is letter-V shaped and has two intersection points with the identity function ($f(z) = z$) can be transformed into (2) with unit threshold by a linear transformation of the overall system [5].

Equation (2) defines a plane, $z = 1$, that separates the two linear half systems. As an aid to intuition, we imagine the z-variable pointing up. The plane $z = 1$ can then the pictured as a "water surface" that separates an "underwater system" ($z \leqq 1$) from an "air system" ($z > 1$).

The letter-V shape of the function $f(z)$ in (2) is the reason that each half-system contains a steady state. The flow of the trajectories in each half system can be written down easily. Each trajectory moves within an invariant 2-dimensional manifold in its own half system. These manifolds can be described explicitly – in reduced (normalized) coordinates, for example.

In the plane $z = 1$, there exists a single line of nontransversal intersection with the flow. It has the equation $y = 1$, since inserting $y = z = 1$ into (1) results in $\dot{z} = 0$. There are no further nontransversal points in the separating plane. Along this line, trajectories of both half systems reaching the plane touch it tangentially. Beyond that line (that is, in the

0340-4811 / 84 / 0400-0342 $ 01.3 0/0. – Please order a reprint rather than making your own copy.

region $y > 1$), all trajectories are welling upwards (from the underwater system into the air system), while in front of it ($y < 1$), all trajectories dive down from the air system into the water system.

3. Poincaré Half Maps and Critical Curves

The trajectories of the underwater half system map the "diving-down region" ($y < 1$) onto the "welling-up region" ($y > 1$) in an almost everywhere bijective fashion. Analogously, the trajectories of the air half system map the welling-up region onto the diving-down region in the same fashion.

Each of the two half maps is described by an implicit function the solution of which gives the next penetration point of the trajectory with the Poincaré surface [5]. This implicit function on the water surface $a + b + 1/(H^3 - 1) = 0$ has the form

$$F(a, b_0, c_0) = 0 \equiv a + b(a, b_0, c_0) + 1/(H^3 - 1)\,, \quad (3)$$

where

$$b\,(a, b_0, c_0) = b_0 \cos\left(\arctan\left(\frac{c_0}{b_0}\right) - QH\,\frac{\log\left(\frac{a}{a_0}\right)}{(H-1)}\right) \cdot \exp\left(\frac{-1 - H/2}{H-1}\log\,(a/a_0)\right), \quad (3\,\mathrm{a})$$

with $a_0 = -b_0 - 1/(H^3 - 1)$.

The reduced variables a, b, c which were here employed are given by the eigenvectors of the original system, $a = (H^2, H, 1)$, $b = (-H^2/2, -H/2, 1)$ and $c = (-QH^2, QH, 0)$, respectively, [2], with parameters $Q = \sin(\pi/3)$ and $H = F^{(1/3)}$ or $G^{(1/3)}$, respectively. One first obtains the next halfstep $a_{n+1/2}$ as a solution to (3), which then gives $b_{n+1/2}$ and $c_{n+1/2}$ by inserting $a_{1/2}$ for a into (3a) or into $c\,(a, b_0, c_0)$, respectively. (The latter function has the r.h.s. of (3a), but with $c_0 \sin$ replacing $b_0 \cos$.) The same equation (Eq. (3) with H corresponding to the other half system) then gives a_{n+1}, and so forth.

A geometric picture of the two half maps can be obtained by means of the following consideration. Each trajectory remains within its own manifold. These manifolds look like rotation-symmetric tree trunks (in the reduced coordinates a, b, c). Their intersection lines with the water surface look like yearly rings [2].

In the simplest case the intersection curve forms a single open curve (of letter-Ω shape). Here the mapping from the diving-down part of this curve onto its own welling-up part is diffeomorphic. There is an "uncritical" fixed point of this mapping, at $y = 1$ [2]. In the case of somewhat "thinner trees", the Omega curve has changed into two separated curves: A thinner tree produces no longer a single intersection curve with the water surface, but two, namely a closed isola and its more or less straight counterpart [1]. Here the corresponding internal mapping has a more complicated topology. One part of the closed isola may be mapped onto another part of the same isola while the rest is mapped onto part of the other, more or less straight, curve. As an example, consider the underwater system with the parameter $F < -8$. Three intersection lines with the water surface $z = 1$, and their internal mappings, are shown in Figure 1.

Now a global 2-dimensional interpretation can be attempted. The set of all "critical points" that divide the different segments of all the yearly rings as shown possess a common property: They all are images (or pre-images, respectively) of a connected "critical" portion of the line $y = 1$. In the case of the underwater half map, the critical portion of the line $y = 1$ is the one where the trajectories touching the "water surface" tangentially are coming from the depth. The critical portion therefore is that part on which $\dot{x} < 1$ (as can be seen by looking at $\dot{z}$ in (1)). Trajectories in a y-neighborhood to that critical portion either switch to the air half system the moment they come out of the water or (if they do not quite make it) dive down back deep into the water immediately in order to make at least one more swing around the tree axis before coming up again.

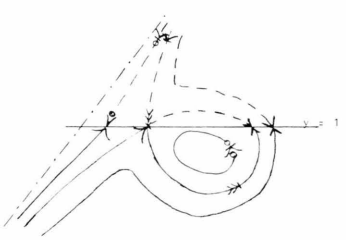

Fig. 1. Typical intersection lines formed by three invariant manifolds of the underwater half system at $G < -8$. Segments mapped by the underwater half map (full lines) onto their images (broken lines) are indicated by arrows and markers as end points. –·–·–· = tree basis ($a = 0$).

In the uncritical portion $x > 1$ of the line $y = 1$, in contrast, neighbors of tangentially touching trajectories remain in the water only for a short time, emerging back into the air close to the line $y = 1$. Therefore, the noncritical portion of the line constitutes a "fixed line" (connected set of fixed points) of the underwater half map. Compare the right-hand portion of $y = 1$ in Figure 1.

Both the image and the pre-image of the critical portion of the line $y = 1$ form "critical curves", as they may be called. In dependence on the system parameter F or G, respectively, the topological structure of these curves shows some variability. In the simplest case, there is a "critical spiral" in the diving-down region, and a "critical fish-hook" in the welling-up region.

Both these critical curves are "separating" in the sense that any two-dimensional regions lying to either side of them are mapped onto disconnected regions by the corresponding half map. More important is the converse of this statement: All regions not traversed by a critical curve are mapped onto a single connected region (in a diffeomorphic fashion except for boundary points). The resulting fragmented and distorted half maps were presented in detail previously [2].

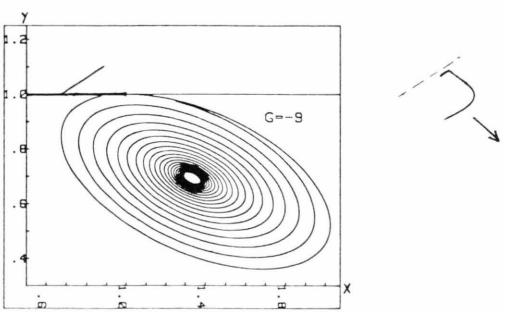

Fig. 2. Critical curves of the underwater half system. The pre-image of the critical (bold) part of the line $y = 1$ is the critical spiral, the image gives a fishbook-shaped critical curve shown once more in the blow-up on the right. (Arrow = direction of magnification.)

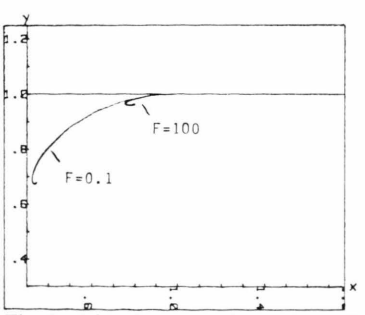

Fig. 3. Critical curves of the air half system. The image of the critical (right hand) part of the line $y = 1$ is the critical spiral. Two critical spirals (for two different values of F) are plotted. The pre-image is a hook-shaped curve lying outside the region of interest.

For one special parameter value, the underwater critical curves are shown in Figure 2. In Fig. 3, analogous curves are presented for the air half system. In the air half system, the critical portion of the line $y = 1$ is that for which $x > 1$, in contradistinction to what holds true for the underwater half system.

4. Composite Maps and Their Chaos

The necessary next step is to combine the two half maps. This leads to the classical Poincaré map which is an almost everywhere bijective map of the diving-down region (or the welling-up region, respectively) back onto itself.

Regions of special interest are those where some kind of recurrent behavior is possible. In the simplest such case there exists a simple fixed point in the Poincaré map (corresponding to a closed trajectory with "period one"). The non-recurrent regions are without much interest – for example, the one lying above the intersection line of the water surface of the air half system. Trajectories in that region are propelled by the air half system toward infinity without returning to the water surface.

In the regions of interest, the critical curves of both half systems can lead to rather complex situations: Imagine Figs. 2 and 3 superimposed. In dependence on the parameters F and G, topologically different composite (Poincaré) maps can be found. Our Eq. (1) as chosen cannot realize all possible topological combinations since we have only one free parameter for each half system. On the other hand, choosing values unequal to unity for some more parameters of (1) may increase the number of possibilities.

In the following, only two combinations will be considered in some detail. Both can appear in the simple system of (1), and both are interesting since they lead to chaotic behavior. The first leads to what may be called "segmentation chaos" since it is born out of a segmentation process generated by the

mapping in question. Under iteration of this Poincaré map, a complicated attractor with a fractal structure [6] can be found.

The second type leads to chaos via continuous (segmentation-free) distortion of a region. This distortion has spiral form. Any spiral map necessarily contains horseshoe-shaped sub-regions. The potentially rich behavior of horseshoe maps, implying the possibility of "basic sets" (that is, chaotic separatrices, in modern parlance), was first expounded by Smale [7].

There is a close connection to the two basic types of chaos that are found in the study of one-dimensional iterations: the discontinuous difference equations, on the one hand, and the continuous (smooth, e.g. parabola-shaped) difference equations, on the other (cf., for example, [8, 9]). Such maps can be considered as "noninvertible limiting cases" to the almost everywhere invertible (2-dimensional) maps of the present system.

In our system, the diving-down part of the region of interest is mapped onto an almost straight, very narrow region by the underwater half map. Sparrow [10] gave an approximation to the system Eq. (1) which leads to a strictly one-dimensional map. Using this method, he found an example of the first type of chaos mentioned above, the segmentation chaos. The continuous (parabola map) chaos has been found without using approximations [5].

In Fig. 4, we present an example for segmentation chaos in the full 2-dimensional Poincaré map. One sees that three segments of the punctured arc in the lower diving-down region (almost one-dimensional) are each mapped onto nearly the full (nearly straight, and also nearly one-dimensional) arc in the upper welling-up part of the Figure. Fig. 5a shows the corresponding apparent one-dimensional map and its time-behavior. One sees no periodic component even over a long time. It should be noted, however, that numerical accuracy per iteration is not higher here than in the usual numerical calculation of chaotic iterations (about 12 digits). What is completely absent, however, is any numerical integration error.

It is worth pointing out that the causation of the second type of chaos possible in (1) is already apparent, in emergent form, from the left-hand part of Fig. 5a. One sees there a little "parabola" hanging down to the right of the three descending segments. By a change of parameters, this parabola can easily be made the center of an attracting box of its own (Figure 5b).

The parabola seen in Fig. 5a (and blown up in Fig. 5b) actually is only the first excursion of a chain of infinitely many, both more and more damped and more and more closely spaced, oscillations. In principle, each of these excursions can be blown up and be shifted to the identity line (by a slight parameter change) in such a way that one obtains a (smaller and smaller) attracting box with chaos. In the limit of the smallest such parabola (with infinite curvature), one has the case that the trajectory moving downward inside the tree axis of the air system is mapped, by the underwater half system, onto the tree basis of the air system again (and from there to the tree axis again by the air system). Such a special trajectory (first leaving and then reapproaching a saddle point) is called homoclinic. According to Shil'nikov [11], homoclinicity to a saddle focus implies presence of a Smale horseshoe (cf. [7]) under certain mild conditions, and hence manifest chaos in many cases. The present case of a Shil'nikov situation arises when in the water surface the pre-image of the (straight) tree basis of the air system, by the underwater system, hits precisely the tree axis of the air system (and hence intersects the whole set of infinitely many windings of the critical spiral of the air system). As a consequence, infinitely many Smale horseshoes of differing sizes (one for each winding of the critical spiral) are formed.

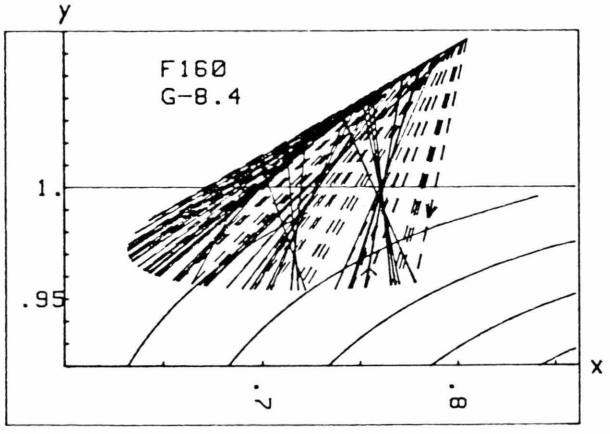

Fig. 4. Two-dimensional Poincaré map. Successive points in the water surface are connected by lines. (Broken lines connect a starting point with $y > 1$ with the subsequent landing (and diving-down) point at $y < 1$; continuous lines connect a diving-down point with the subsequent welling-up (and starting) point.)

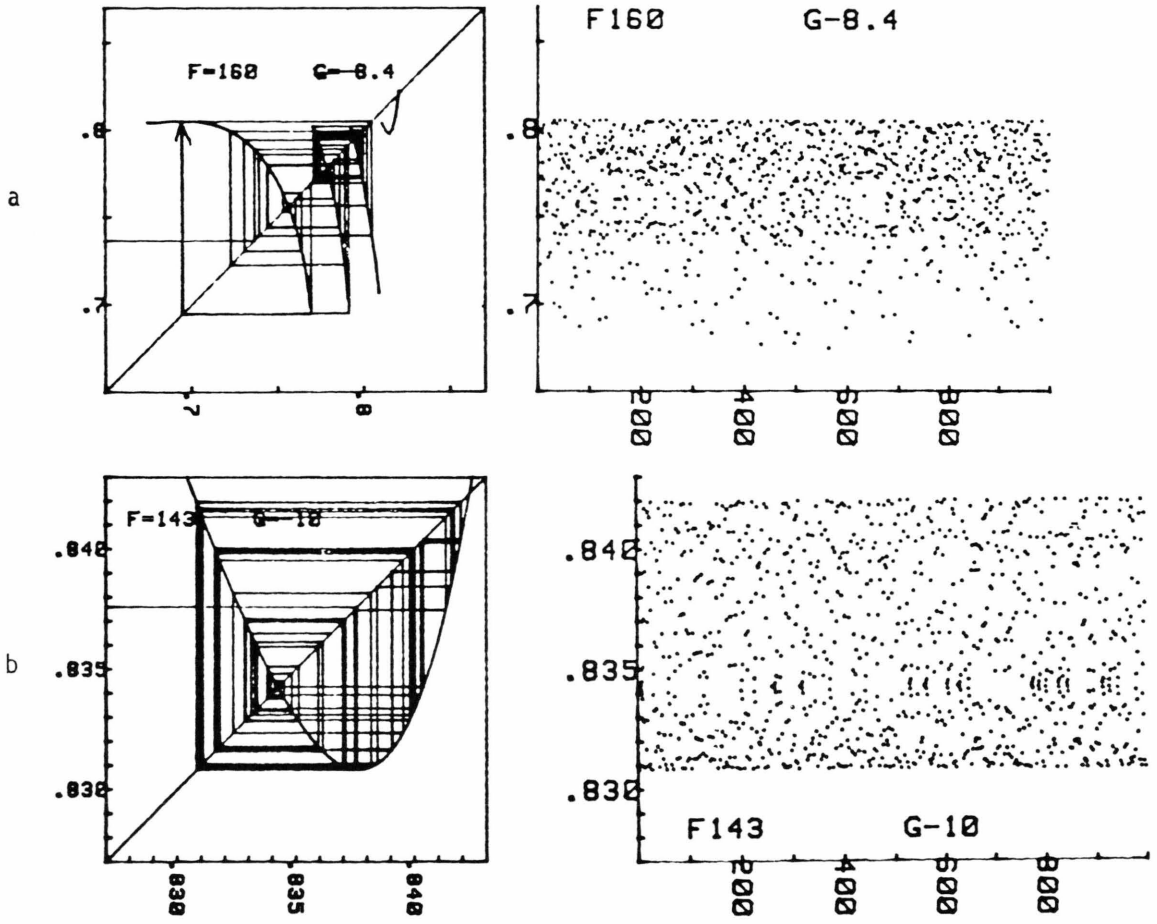

Fig. 5. Seemingly one-dimensional Poincaré maps: The one-dimensional variable plotted is the x-component of the map of Fig. 4 (in the case of the trajectories), and of the first image of the straight line formed by the intersection of the underwater tree basis with the water surface (in the case of the reference curves entered for comparison). The time-evolution of one trajectory is also shown. a) Discontinuous chaos. b) Parabola chaos.

Figure 5b thus shows the first in a series of smaller and smaller chaotic attractors that are formed as a path in parameter space leading up to Shil'nikov's situation is followed. In the limit, the last such chaotic attractor has shrunk to a point and disappeared. This seems to be typical for one of the two basic Shil'nikov situations that can exist (as each other's time inverses). In the present case it is the saddle focus of the air system that is involved, with its *contracting* two-dimensional manifold (tree basis). Therefore, no manifest chaos can exist in the limit (unless time is inverted). Whether or not the other type (which would have to be based on the underwater saddle focus) is also possible in (1), with some of the unit parameters nonunity, is presently open.

5. Discussion

Two types of chaos were demonstrated (one for the first time) in a piecewise linear system of C^1 type. (Note that trajectories are C^1 – "once differentiable" – if the right hand sides are C^0 – continuous".) This is the most "natural" class of piecewise linear systems since they approximate other (ordinary) nonlinear systems without a sharp "bent" (and without being singular). The only other class of analytically tractable ordinary differential equations with manifest chaos is the class of three-variable singular-perturbation type differential equations, in the limit the singular-perturbation parameter goes to zero (so that the pertinent, alternatively applying, subsystems are actually two-dimensional – and

hence rather singular – among the set of all 3-variable systems). See [12, 13] (and [14] for a review).

Historically, there exists one particular piecewise linear system, the Danziger-Elmergreen equation [3] of hormonal regulation, for which the hypothesis that it might possess nontrivial solutions is in the literature for quite a while [4]. This equation actually constitutes a special case to (1) (with $F = 0$ and the unit parameters in the second and third line non-unity). We were so far unable to verify theorem 8 of Cronin's paper [4] in which the possibility of a nonperiodic motion ("Birkhoff recurrence") in the Danziger-Elmergreen equation is asserted. It still appears possible that by varying further parameters in (1), an appropriate set of parameters generating quasiperiodicity and/or chaos can be found.

Piecewise linear chaos is gaining momentum. A first chaos-producing version of (1) was proposed in 1978 [15]. It was C^0 and was therefore accompanied by a less elegant (3-piece) C^1 version to make it more realistic. More recently, Kahlert [16] also described a piecewise-linear chaos-producing 3-variable autonomous system of the C^0 type. (For two non-autonomous C^0 examples, see [17, 18].) The method of Poincaré half maps [2] is very useful also with such equations [16]. It even appears promising to use this method in order to systematically derive all possible chaos-generating piecewise-linear 3-variable systems (of both C^0 and C^1 type) that have one planar threshold. One further C^1 system that is at least as simple as Eq. (1) has already been found [19].

Let us conclude the discussion with an outlook on things to come – that is, on the behavior of more than 3-variable, piecewise-linear systems. Here at first the infinite-dimensional special case of (1) comes to mind. If further linear phase-shifting variables are added to the two present in (1) such as to yield an infinitely long chain, the resulting equation can be written more compactly in the form

$$\dot{x} = -x + f(x_{t-1}) \,. \tag{4}$$

In such a functional (or delay-type, respectively) differential equation, chaos was first found by Mackey and Glass [20]. One readily sees that by multiplying the left-hand side of (4) by ε, one in the limit ε approaches zero obtains a difference equation, namely

$$x_{t+1} = f(x_t), \tag{5}$$

which is potentially chaos-producing. This may be taken as evidence that in the original equation (1), chaos also should be possible for sufficiently large n. Actually, this is how (1) was originally arrived at in the present approach [15]: as providing an extremal simplification to (4). (The same reasoning independently lead Sparrow [21] to his close to piecewise-linear nonlinear 50-variable phase-shift system with chaos.) Equation (1) with $n = 4$ indeed still produces chaos (for example, when $F = 30$ and $G = -4.3$ [5]), continuing to do so through larger n.

However, the infinite-dimensional case ((4) and (5)) was mentioned for an additional reason. One easily sees that (5) (and hence (4)) contains not just ordinary chaos (with one single direction of repetitive stretching and folding-over, that is, one positive Lyapunov characteristic exponent; cf. [14]), but infinite hyper chaos (that is, chaos with infinitely many such directions and exponents). The reason lies in the fact that (5) has a continuous (t) rather than discrete (n) subscript. This means that this difference equation needs infinitely (uncountably) many initial points specified (a whole unit interval), one for each of its equally many uncoupled chaotic regimes. If now ε in (4) (as mentioned) is rendered finite (though arbitrarily small) rather than zero, the order of the chaos can be expected to drop down to finite values immediately – but not quite down to unity. This conjecture is in accordance with recent numerical findings [22] which independently suggest the presence of a high-dimensional attractor in (4) for certain parameters.

Therefore, (1) with $n = 4$ can be expected to produce *higher* chaos (with 2 positive exponents) already; and so forth. Since the method of Poincaré half maps [2] can be applied to arbitrary dimensions, the next step will be to show that for (1) with $n = 4$, again an implicit equation (like (3)) can be presented for each half map, but this time in 3 variables. Techniques how to analyze such equations economically for the presence of "hyper horseshoes" [15] and their attendant homoclinicities have yet to be developed. Hereby, focusing on homoclinic points in state space may again provide one strategy for search.

Acknowledgements

We thank Claus Kahlert and Igor Gumowski for discussions.

[1] O. E. Rössler, The Gluing-together Principle and Chaos, in: Nonlinear Problems of Analysis in Geometry and Mechanics (M. Attaia, D. Bancel, and I. Gumowski, eds.), Pitman, Boston-London, 1981, pp. 50–56. Cf. also R. Rössler, F. Götz, and O. E. Rössler, Biophys. J. **25,** 216a (1979) (abstract).
[2] B. Uehleke and O. E. Rössler, Z. Naturforsch. **38a,** 1107 (1983).
[3] L. Danziger and G. L. Elmergreen, Bull. Math. Biophys. **18,** 1 (1956).
[4] J. Cronin, Bull. Math. Biol. **35,** 689 (1973).
[5] B. Uehleke, Chaos in einem stückweise linearen System: Analytische Resultate, Ph.D. thesis, University of Tübingen, 1982.
[6] B. Mandelbrot, Form, Chance, and Dimension, Freeman, San Franzisko 1977.
[7] S. Smale, Bull. Amer. Math. Soc. 173, 747 (1967).
[8] R. M. May and G. F. Oster, Am. Naturalist **110,** 573 (1976).
[9] B. Uehleke, Chaos in diskreten und kontinuierlichen Dynamischen Systemen, Diploma Thesis, University of Tübingen, 1979.
[10] C. Sparrow, J. Math. Anal. Appl. **83,** 275 (1981).
[11] L. P. Shil'nikov, Sov. Math. Dokl. **6,** 163 (1965).
[12] O. E. Rössler, Z. Naturforsch. **31a,** 259 (1976).
[13] F. Takens, Springer Lect. Notes Math. **535,** 237 (1976).
[14] O. E. Rössler, Z. Naturforsch. **38a,** 788 (1983).
[15] O. E. Rössler, Chaos and hyperchaos in nonlinear differential equations. Paper presented at the "Workshop on Systems Described by Ordinary Differential Equations", Cambridge, England, June 26–28, 1978.
[16] C. Kahlert, Chaos in a piecewise linear boundary value problem. To be published.
[17] J. N. Schulman, Phys. Rev. **28A,** 477 (1983).
[18] J. M. T. Thompson, Proc. Roy. Soc. London **A, 387,** 407 (1983).
[19] In preparation.
[20] M. C. Mackey and L. Glass, Science **197,** 287 (1977).
[21] C. Sparrow, A strange attractor in a single-loop feedback system. Paper presented at the "Workshop on Systems Described by Ordinary Differential Equations", Cambridge, England, June 26–28, 1978.
[22] J. D. Farmer, Physica **4D,** 366 (1982).